

# Positive and negative magnetocapacitance in magnetic nanoparticle systems

G. Lawes<sup>1,2</sup>, R. Tackett<sup>1</sup>, O. Masala<sup>3</sup>, B. Adhikary<sup>1</sup>, R. Naik<sup>1</sup>, and R. Seshadri<sup>3</sup>

<sup>1</sup> *Department of Physics and Astronomy, Wayne State University, Detroit, MI 48201*

<sup>2</sup> *Los Alamos National Laboratory, Los Alamos, New Mexico 87545 and*

<sup>3</sup> *Materials Department and Materials Research Laboratory,  
University of California, Santa Barbara, CA 93106*

(Dated: September 5, 2018)

The dielectric properties of  $\text{MnFe}_2\text{O}_4$  and  $\gamma\text{-Fe}_2\text{O}_3$  magnetic nanoparticles embedded in insulating matrices were investigated. The samples showed frequency dependent dielectric anomalies coincident with the magnetic blocking temperature and significant magnetocapacitance above this blocking temperature, as large as 0.4% at  $H = 10\text{ kOe}$ . For both samples the magnetic field induced change in dielectric constant was proportional to the square of the sample magnetization. These measurements suggest that the dielectric properties of magnetic nanoparticles are closely related to the disposition of magnetic moments in the system. As neither bulk  $\gamma\text{-Fe}_2\text{O}_3$  nor  $\text{MnFe}_2\text{O}_4$  are magnetoelectric materials, this magnetodielectric coupling is believed to arise from extrinsic effects which are discussed in light of recent work relating magnetoresistive and magnetocapacitive behavior.

PACS numbers: 75.50Tt, 77.22.Gm, 77.84.Lf

Given the renewed activity in investigating materials exhibiting strongly coupled electric and magnetic properties,[1] there is great interest to develop new systems with large magnetocapacitive couplings. In this contribution, we experimentally explore the possibility of developing new magnetodielectric materials using magnetic nanoparticles, and discuss our results in the context of a magnetoresistive origin for magnetocapacitive couplings.[2]

Nanoscale composites can often show large interactions between the magnetic and electronic properties. For example, in composite materials formed by depositing  $\text{CoFe}_2\text{O}_4$  nanopillars in a  $\text{BaTiO}_3$  matrix, the elastic coupling between the different constituents gives rise to sizable magnetoelectric coupling.[3] Here we focus on magnetic nanoparticle systems, whose magnetic properties are well understood in terms of thermally activated spin flipping,[4] and yet have not been much studied from the viewpoint of the relationship between dielectric and magnetic properties.[5, 6, 7] Very recent work on  $\epsilon\text{-Fe}_2\text{O}_3$  nanoparticles show large magnetocapacitive couplings, which are attributed to intrinsic magnetoelectric couplings in this material[7].

The systems investigated here are magnetic nanoparticles of  $\gamma\text{-Fe}_2\text{O}_3$  and  $\text{MnFe}_2\text{O}_4$  embedded in insulating matrices. The magnetic properties of these nanoparticle systems are well understood.[8, 9] The  $\text{MnFe}_2\text{O}_4$  nanoparticles were prepared through the high-temperature decomposition of metal acetylacetonate precursors, and are capped with long chain organic molecules, which form the insulating matrix.[10] The nanoparticles were characterized using X-ray diffraction (XRD) and electron microscopy, showing they are crystalline with an average diameter of 4.6 nm. The  $\gamma\text{-Fe}_2\text{O}_3$  nanoparticles were prepared through a set of sequential reactions described elsewhere (ref. [11]). XRD characterization show these nanoparticles are crystalline and electron microscopy indicated an average particle diam-

eter of 5.5 nm.

AC magnetic susceptibility measurements were performed on a Quantum Design PPMS between  $T = 2\text{ K}$  and  $T = 300\text{ K}$  at magnetic fields up to  $H = 10\text{ Oe}$ . In order to measure the dielectric properties of these materials, we cold pressed approximately 50 mg of sample into a thin, solid pellet. For the  $\text{MnFe}_2\text{O}_4$  sample, we deposited gold electrodes on opposite sides of this pellet, and attached platinum leads using silver epoxy. For the  $\gamma\text{-Fe}_2\text{O}_3$  sample electrodes were fashioned and the leads attached using silver epoxy. We mounted the sample in the PPMS using a custom designed probe and measured the complex dielectric constant with measuring frequencies between  $\omega_m/2\pi = 5\text{ kHz}$  and  $\omega_m/2\pi = 1\text{ MHz}$  using an Agilent 4284A LCR meter.

The upper panels of FIG. 1 show the temperature dependence of the out-of-phase AC magnetic susceptibility  $\chi''$  (loss component) of the  $\text{MnFe}_2\text{O}_4$  and  $\gamma\text{-Fe}_2\text{O}_3$  nanoparticles, and the lower panels show the temperature dependence of out-of-phase dielectric loss tangent  $\epsilon''$  recorded at  $H = 1\text{ kOe}$ . The data were acquired at different measurement frequencies. In the Néel-Brown model,[4] the characteristic relaxation time for the magnetization of each (non-interacting) nanoparticle is given by:

$$\tau = \tau_0 \exp(E_A/k_B T) \quad (1)$$

where  $\tau$  is the relaxation time for the magnetic moment,  $\tau_0$  is a microscopic timescale (normally close to  $10^{-9}$  seconds),  $E_A$  is the energy barrier to moment reversal (taken to be the product of nanoparticle volume  $V$  and magnetocrystalline anisotropy  $K$ ;  $E_A = KV$ ), and  $T$  the temperature. At high temperatures,  $\tau$  will be smaller than the characteristic measuring time – the nanoparticles are in the superparamagnetic state – while at low temperatures  $\tau$  will be large, and the nanoparticle moments are

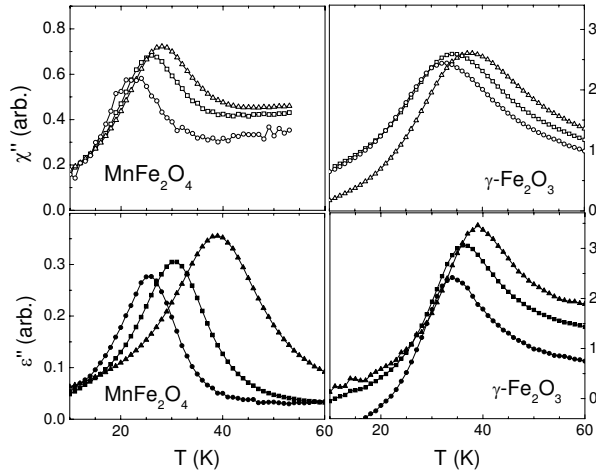


FIG. 1: Upper left panel: Out-of-phase component of magnetic susceptibility of the 4.6 nm  $\text{MnFe}_2\text{O}_4$  nanoparticles plotted versus temperature at  $H = 1$  kOe. The AC measuring frequencies are: 100 Hz (leftmost curve), 3 kHz (middle curve), and 10 kHz (rightmost curve). Lower left panel: Out-of-phase dielectric component of the 4.6 nm  $\text{MnFe}_2\text{O}_4$  nanoparticles plotted versus temperature at  $H = 1$  kOe. Frequencies: 5 kHz (leftmost curve), 50 kHz (middle curve), and 1 MHz (rightmost curve). Upper right panel: Out-of-phase component of magnetic susceptibility of the 5.5 nm  $\gamma\text{-Fe}_2\text{O}_3$  nanoparticles plotted versus temperature at  $H = 1$  kOe. Frequencies: 1 kHz (leftmost curve), 3 kHz (middle curve), and 10 kHz (rightmost curve). Lower right panel: Out-of-phase dielectric component of the 10 nm  $\gamma\text{-Fe}_2\text{O}_3$  nanoparticles plotted versus temperature at  $H = 1$  kOe. Frequencies: 10 kHz (leftmost curve), 30 kHz (middle curve), and 100 kHz (rightmost curve).

thermally blocked. The peak in  $\chi''$  occurs at the temperature where  $\tau\omega_m = 1$ , with  $\tau$  determined from Eq. 1, and  $\omega_m$  is the AC measuring frequency.

The lower panels in FIG. 1 show that the loss component of the dielectric constant of  $\text{MnFe}_2\text{O}_4$  and  $\gamma\text{-Fe}_2\text{O}_3$  exhibit peaks at temperatures commensurate with the transition from the high temperature superparamagnetic regime to the low temperature blocked state. This argues that the dielectric properties of the  $\text{MnFe}_2\text{O}_4$  and  $\gamma\text{-Fe}_2\text{O}_3$  nanocomposites are sensitive to the magnetic dynamics. We believe these nanoparticles are rigidly fixed within the insulating matrix at all temperatures, so this dielectric anomaly does not arise from any physical motion of the nanoparticles. This observation that the peaks in  $\chi''$  and  $\epsilon''$  in both systems show as correspondence is significant because it demonstrates that this coupling between magnetic and dielectric properties of nanoparticles is apparently general feature of such systems, and does not depend on any specific material property.

Furthermore, if the underlying mechanism for both the magnetic and dielectric relaxation is thermally activated moment reversal (Eq. 1) in individual nanoparticles, the magnetic and dielectric data should fall on the same

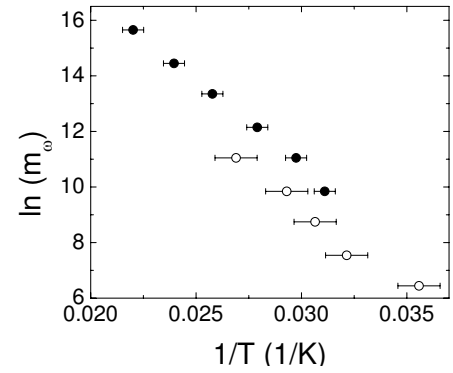


FIG. 2: Natural logarithm of the measuring frequency plotted against the inverse temperature of the loss peak for  $\gamma\text{-Fe}_2\text{O}_3$ . The open symbols were extracted from the magnetization data, the solid symbols from the dielectric data.

curve. Figure 2 shows the Arrhenius curve for the low temperature relaxation feature for  $\gamma\text{-Fe}_2\text{O}_3$  determined using magnetic and dielectric measurements on the same plot. Within experimental error, these two curves agree very well, giving an activation energy of  $E_A = 710$  K. This agreement provides very strong evidence that the anomalies observed in the dielectric constant of these systems have their origins in the magnetic properties of the nanoparticles.

As a final probe of the magnetodielectric properties of these  $\text{MnFe}_2\text{O}_4$  and  $\gamma\text{-Fe}_2\text{O}_3$  systems, we investigated the magnetic field dependence of the dielectric constant at fixed temperature. The upper panel of Figure 3 plots the fractional change in dielectric constant of the  $\text{MnFe}_2\text{O}_4$  composite as a function of magnetic field. The dielectric constant of  $\text{MnFe}_2\text{O}_4$  decreases by almost 0.1% when a magnetic field of  $H = 10$  kOe is applied at  $T = 70$  K. The lower panel of Figure 3 shows the relative change in dielectric constant of  $\gamma\text{-Fe}_2\text{O}_3$  as a function of magnetic field at several different temperatures. Well above the blocking temperature, at  $T = 200$  K and  $T = 300$  K, the dielectric constant increases by over 0.4% in a field of  $H = 10$  kOe. However, at  $T = 20$  K and  $T = 100$  K the dielectric constant is effectively independent of magnetic field, at least below  $H = 10$  kOe. The square of the magnetization is plotted as the solid symbols in Fig. 4, at  $T = 70$  K for  $\text{MnFe}_2\text{O}_4$ , and  $T = 300$  K for  $\gamma\text{-Fe}_2\text{O}_3$ . For both these nanoparticle samples, the fractional change of the magnetic field induced change in the dielectric constant can be well approximated by:

$$\frac{\Delta\epsilon}{\epsilon} = \alpha M^2. \quad (2)$$

A similar dependence of the change in dielectric constant on the square of the magnetization has been observed in several bulk materials.[12, 13, 14] For  $\text{MnFe}_2\text{O}_4$ , nanoparticles,  $\alpha$  is small and negative, while for  $\gamma\text{-Fe}_2\text{O}_3$ ,  $\alpha$  is roughly a factor of 20 larger and positive.

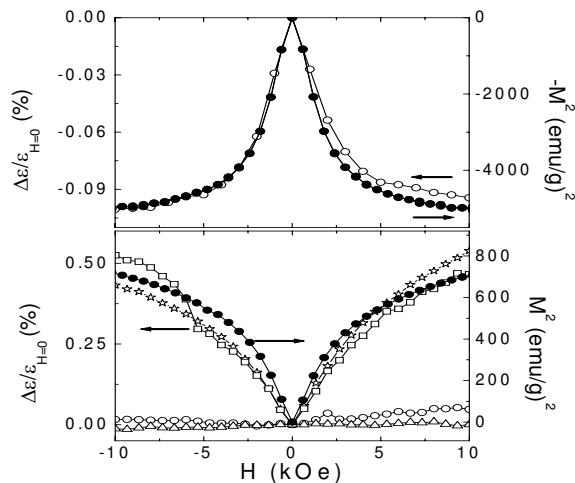


FIG. 3: Upper Panel: Relative change in the dielectric constant of the 4.6 nm  $\text{MnFe}_2\text{O}_4$  nanoparticle system as a function of external magnetic field, measured at  $T = 70$  K and a frequency of 1 MHz. Solid symbols plot the negative of the square of the sample magnetization at  $T = 70$  K. Lower Panel: Relative change in the dielectric constant of the 5.5 nm  $\gamma\text{-Fe}_2\text{O}_3$  nanoparticle system as a function of external magnetic field, at temperatures from  $T = 20$  K to  $T = 300$  K, as indicated on the figure. The measuring frequency was 300 kHz. The solid symbols plot the square of the sample magnetization at  $T = 300$  K.

These results can be well understood in terms of a recent proposal suggesting that inhomogeneous systems with large magnetoresistance should also show significant magnetocapacitive effects.[2] In this framework, the Maxwell-Wagner capacitor model is used to predict the dielectric response of magnetoresistive materials. The measured capacitance depends on the resistance of the bulk-like and interfacial layers in the system. If the resistance of these layers is changed in a magnetic field, the capacitance will change as well, leading to a magnetodielectric shift. It has been established

that magnetic nanoparticles often show magnetoresistive properties,[15, 16] attributed to spin-polarized tunneling, so magnetic nanoparticles may be expected to show such magnetodielectric effects. Our data agree qualitatively with several predictions of this model: the shift in dielectric constant is proportional to the square of the magnetization, and we observe both *positive* ( $\gamma\text{-Fe}_2\text{O}_3$ ) and *negative* ( $\text{MnFe}_2\text{O}_4$ ) magnetocapacitance. We can also compare our results with quantitative predictions of the model. With the same assumptions made by Catalan[2] together with published values for the magnetoresistance of  $\gamma\text{-Fe}_2\text{O}_3$  (-2% magnetoresistance at  $H = 10$  kOe[15]) the predicted magnetocapacitance for  $\gamma\text{-Fe}_2\text{O}_3$  at 300 K is on the order of 1%. This is comparable to our observed value of 0.4%.

In conclusion, we have investigated the dielectric properties of  $\text{MnFe}_2\text{O}_4$  and  $\gamma\text{-Fe}_2\text{O}_3$  magnetic nanoparticle composites. Both of these materials exhibit a peak in dielectric loss at the magnetic blocking temperature, and both show a field dependent dielectric constant above the blocking temperature which varies as the square of the sample magnetization. Our data, including the different signs for the magnetocapacitance in  $\gamma\text{-Fe}_2\text{O}_3$  and  $\text{MnFe}_2\text{O}_4$ , can be well understood using a recently proposed model for magnetodielectric coupling in magnetoresistive systems.[2] These results are significant because they provide experimental confirmation for composite magnetodielectric systems with magnetoresistive constituents, with electronic rather than elastic magnetocapacitive couplings. Furthermore, our results emphasize that magnetodielectric anomalies in themselves are not proof of multiferroic behavior.[2]

The work at Los Alamos National Laboratory was supported by the LDRD program. We acknowledge helpful conversations with A. P. Ramirez. OM and RS acknowledge support from the NSF Chemical Bonding Center (Chemical Design of Materials) under Award No. CHE-0434567, and from the Donors of the American Chemical Society Petroleum Research Fund.

- 
- [1] N. A. Hill, *J. Phys. Chem. B* **104**, 6694 (2000).
  - [2] G. Catalan, cond-mat/0510313
  - [3] H. Zheng, *et al.*, *Science* **303**, 661 (2004).
  - [4] W. F. Brown, *Phys. Rev.* **130**, 1677 (1963).
  - [5] R. Pelster, A. Spanoudaki, and T. Kruse, *J. Phys. D: Appl. Phys.* **37**, 307 (2004).
  - [6] N. N. Mallikarjuna, S. K. Manohar, P. V. Kulkarni, A. Venkataraman, and T. M. Aminabhavi, *J. Appl. Polymer Sci.* **97**, 1868 (2005).
  - [7] M. Gich, C. Frontera, A. Roig, J. Fontcuberta, E. Molins, N. Bellido, Ch. Simon, and C. Fleta, cond-mat/0509104
  - [8] A. F. Bakuzis, P. C. Morais, and F. Pelegrini, *J. Appl. Phys.* **85**, 7480 (1999).
  - [9] J. L. Dormann, *et al.*, *J. Magn. Magn. Mater.* **183**, L255 (1998).
  - [10] O. Masala and R. Seshadri, *Chem. Phys. Lett.* **402**, 160 (2005).
  - [11] E. Kroll, F. M. Winnik, and R.F. Ziolo, *Chem. Mater.* **8**, 1594 (1996).
  - [12] T. Katsufuji and H. Takagi, *Phys. Rev. B* **64**, 054415 (2001).
  - [13] G. Lawes, *et al.*, *Phys. Rev. Lett.* **91**, 2572081 (2003).
  - [14] T. Kimura, S. Kawamoto, I. Yamada, M. Azuma, M. Takano, and Y. Tokura, *Phys. Rev. B*, **67**, 180401 (2003).
  - [15] J. Tang, L. Feng, and J. A. Wiemann, *Appl. Phys. Lett.* **74**, 2522 (1999).
  - [16] K. Liu *et al.*, *J. Appl. Phys.* **93**, 7951 (2002).